Penspen Integrity
Units 7-8
St. Peter's Wharf
Newcastle upon Tyne
NE6 1TZ
United Kingdom

Telephone: +44 (0)191 238 2200
Fax: +44 (0)191 275 9786
Email: integrity.ncl@penspen.com
Website: www.penspenintegrity.com

PIPELINE FAILURE: THE ROLES PLAYED BY CORROSION, FLOW AND METALLURGY

Dominic Paisley
BP Exploration Alaska
Prudhoe Bay, AK 99734, USA
paisledm@bp.com

Nathan Barrett
BP Exploration Wytch Farm
Poole, Dorset UK
barretn@bp.com

Owen Wilson
Andrew Palmer & Associates
40 Carden Place, Aberdeen UK
owen.wilson@penspen.com

ABSTRACT

Carbon dioxide corrosion has been widely studied in the field and laboratory. It is recognized that flow regime and metallurgy are important factors that influence in-situ corrosion rates but there are relatively few documented case studies that are able to separate the individual contributions of corrosion, flow regime and metallurgy on the observed corrosion damage. This paper deals with failure of a pipeline where high quality inspection data together with comprehensive as-built records and stable production conditions allowed the separate influences of flow and metallurgy on corrosion to be studied. The flow regimes in the pipeline ranged from low velocity, stratified flow to high velocity, slug flow. The inspection data showed that the affect of turbulent flow was to increase the frequency of corrosion pits and, in the case of weld corrosion, the mean corrosion rate. The pipeline was constructed from two grades of steel and welded using two types of welding consumable. One grade of pipeline steel corroded at a significantly higher rate and with a higher frequency of corrosion pits than another, apparently similar steel. However, no significant relationship was found between weld metallurgy and corrosion rate or frequency.

INTRODUCTION

Wytch Farm oilfield is located on England's South Coast and is the largest onshore oilfield in Western Europe. In 1997, one of the Wytch Farm production pipelines failed due to internal corrosion. After repair, the pipeline was returned to service but failed again, almost immediately. The failure locations were significantly different in terms of their metallurgy as well as the flow regimes. The second failure prompted a thorough re-assessment of the condition of the pipeline. This involved large scale excavations for inspection and repairs as well as re-analysing intelligent pig data gathered several months earlier. These data, combined with knowledge of the materials of construction, flow regimes and fluid properties, produced a rare insight in to the relationships between metallurgy, flow regime and the corrosion mechanism.

BACKGROUND INFORMATION

Pipeline Construction Details

The Wytch Farm Gathering Station receives oil from remote well sites via a number of pipelines, ranging in size from 89 mm to 324 mm outside diameter. The routing of each pipeline takes it via several well sites, collecting fluids from each one i.e. a trunk and lateral system. These in-field pipelines vary in length from a few hundred metres to 6.4 km.

The 10" Wytch Farm pipeline was installed in three sections by three different contractors during 1987/88, including a 1,100 m long directionally drilled section of pipeline which passes underneath Poole Harbour. It was commissioned in 1990. The pipeline is unusual in that it is constructed from two different grades of linepipe, API 5L Grades B and X42. These were generally arranged in sections but some linepipe spools were distributed randomly along the pipeline length. Both grades of linepipe were produced by the seamless process, of the same nominal wall thickness (WT - 7.8 mm) and produced by the same manufacturer.

High quality as-built records allowed the location of each linepipe spool to be determined. Each construction contractor used a different welding procedure; two of the contractors used similar GMn welding consumables, while the third used a consumable containing 1% Ni. Again, the as-built records allowed the contractor responsible for each weld to be identified.

Figure 1 shows the wellsites and the topography of the pipeline, including the harbour crossing from Wellsite L to Wellsite F. Table 1 gives some general information about the pipeline.

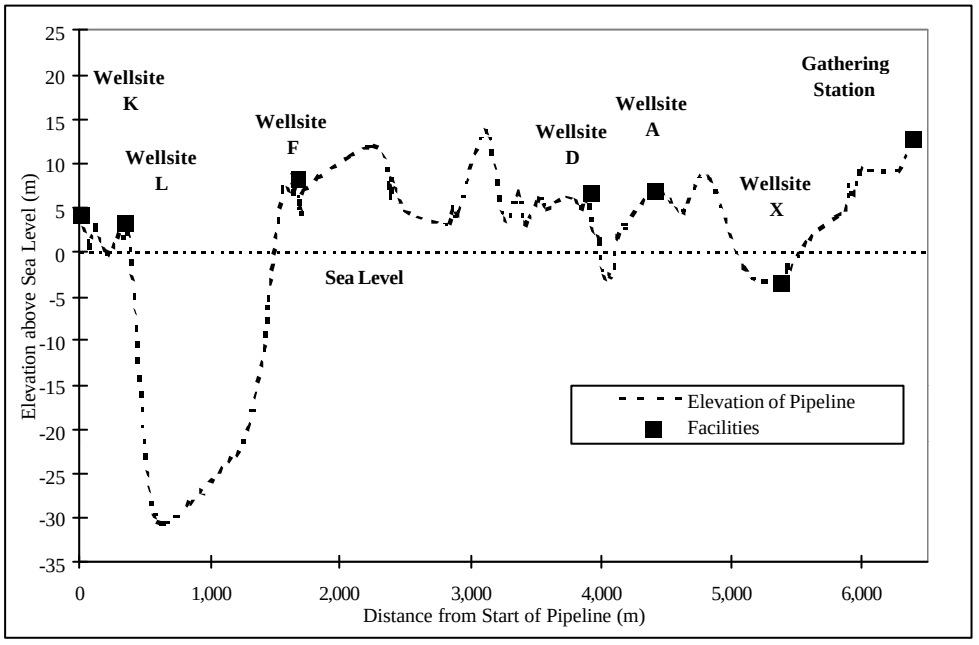

Figure 1: Topography and general arrangement of facilities along the pipeline

TABLE 1
PIPELINE DETAILS

PARAMETER	VALUE
Length	6.4 km
Diameter	273.1 mm (10.75")
Wall thickness (WT)	7.8 mm (0.307")
Material grades	API 5L Grade B and X42
Linepipe type Pre-fabricated bend grade	Seamless X52
Weld consumables	C-Mn and 1% Ni
Design pressure	3.5 MPa
Design temperature	- 5 to 70°C

Flow Regimes

The pipeline is a constant diameter trunk line, connecting six wellsites to the Gathering Station. Although fluid properties from each wellsite are similar, the addition of fluids at successive wellsites and the gas expansion due to pressure drop combine to produce significantly different flow regimes along the pipelines length. Based on multiphase flow regime modelling, the flow regimes range from stratified flow at the inlet of the pipeline at approximately 1 m/s to slug flow, bordering on annular flow at 10 m/s at the outlet. Acoustic monitoring at the outlet confirms the presence of slug flow in this section. The pipeline also varies in elevation by 45 metres - see Figure 1 and this induces changes in the flow regime, discussed later.

DAMAGE DISCOVERED

A high resolution Magnetic Flux Leakage (MFL) intelligent pig was used to inspect the pipeline in late 1996, and the results showed internal corrosion along the length of the pipeline, totalling 281 defects. The frequency of corrosion defects increased towards the Gathering Station, particularly downstream of Wellsite X - see Figure 2. The defects were believed at that time to be restricted mainly to pipebody defects, with only limited indications of corrosion within the girth welds.

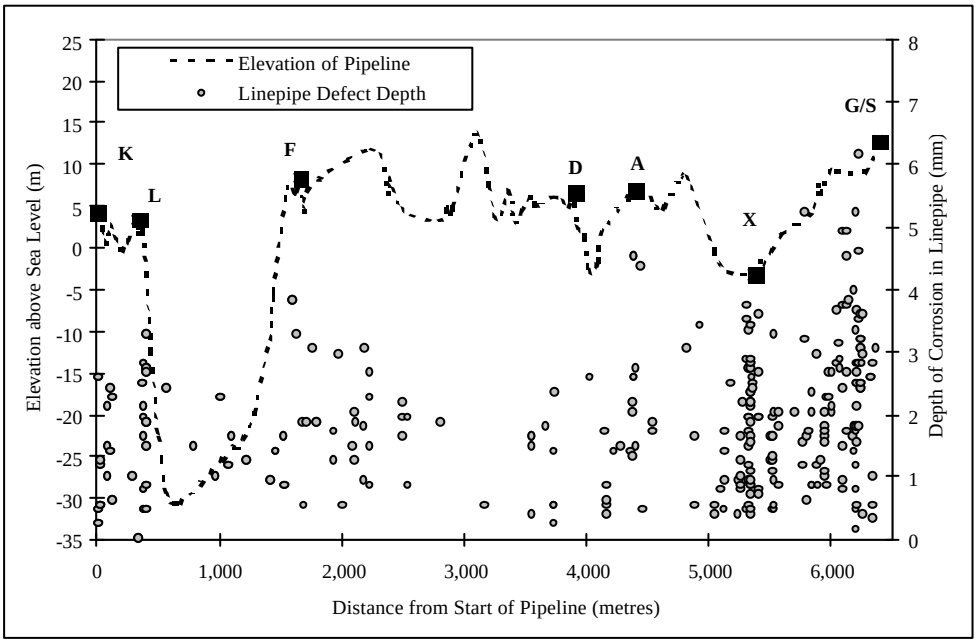

Figure 2: Distribution and Depth of Pipebody Defects Along the Pipeline

In June 1997 two failures occurred within a short space of time, one located at the upstream end of the line close to Wellsite K and one on the downstream end of the line within the boundary of the Gathering Station. The failures were caused by pitting corrosion at the girth welds. Small diameter (circa 10 mm) pits were found to be located entirely on the weld, centred around the cap. The intelligent pig inspection had given no indication of the presence of these features (small corrosion features in welds are typically difficult to identify with MFL techniques).

Manual inspection using gamma radiography and compression wave and Time of Flight Diffraction ultrasonic thickness (UT) measurements revealed widespread girth weld corrosion. Approximately 30% of the pipeline girth welds were excavated and inspected. Improved interpretation of the intelligent pig data, based on results gathered by the manual inspection program enabled a complete picture of the condition of the pipeline to be generated. The analysis of weld corrosion was semi-quantitative, placing corroded welds in to four categories: "Clean welds", "less than 25% wall loss", "25% to 60% wall loss" and "greater than 60% wall loss" These data are shown in Figure 3. For clarity, they are plotted against discrete percentages of wall thickness as shown in Table 2.

TABLE 2
THE CATEGORIES USED TO DESCRIBE WELD CORROSION

CATEGORY OF WELD DEFECT	PLOTTED AS
Clean weld	Not shown
Less than 25% wall loss	25%
25% to 60% wall loss	50%
Greater than 60% wall loss	75%

Figure 3 shows that the distribution of corroded welds follows a similar distribution to the pipebody defects i.e. increasing in frequency towards the Gathering Station. In this case, the effect is more significant as there were virtually no defective welds between the pipeline inlet and kilometre point (KP) 4.0 while there were significant numbers of pipebody defects in all sections. Also, the weld defects in upstream sections were less severe than those in downstream sections.

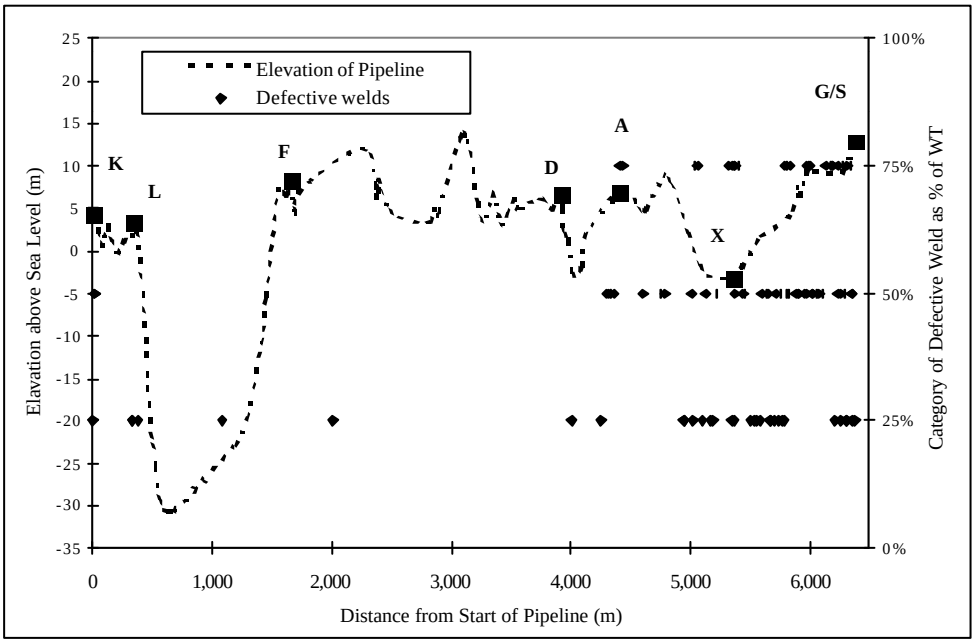

Figure 3: Distribution and Severity of Girth Weld Corrosion Defects Along the Pipeline

CORROSION MECHANISM

Determining the corrosion mechanism is critical if effective control procedures are to be established. The production fluid at Wytch Farm is a sweet, light crude oil and the field had been in production for circa seven years at the time of failure. Investigations into corrosion mechanisms in the field are often complicated by changing field conditions but not in this case as the produced fluid composition had remained essentially constant. The water cut had remained constant at approximately 30%. There was also no evidence of seawater breakthrough, scaling, reservoir souring or bacterial contamination of the pipeline. Also, no production chemicals such as scale inhibitor or corrosion inhibitor had been used. These factors significantly simplified the failure investigation. The fluid properties are shown in Table 3.

TABLE 3
FLUID PROPERTIES

PARAMETER	VALUE
Temperature (inlet to outlet)	65 to 58°C
Pressure (inlet to outlet)	2.8 to 0.8 MPa
CO_2 (gas phase)	0.5 mole%
H_2S (gas phase)	< 10 ppm
Water cut	30%
Bicarbonate concentration	40 ppm
Acetate concentration.	100 ppm
Predicted pH	4.5

The corrosion defects were small, discrete pits (5 to 15 mm diameter). The shape and size were similar in linepipe and weld regions and there was no preferential attack of the heat affected zone. Pits that initiated at the weld root tended to remain in the weld metal, growing in a semi-spherical manner.

Viable corrosion mechanisms for unstabilized crude oil pipelines are:

1. Microbially induced corrosion
2. Hydrogen sulphide corrosion
3. Carbon dioxide corrosion

Microbially induced corrosion (MIC) was ruled out as bacterial surveys of solids samples taken after maintenance pigging failed to detect bacteria. Also, the worst corrosion damage occurred in sections of the pipeline where fluid velocities approached 10 m/s, whereas MIC is typically associated with low velocity (below 1 m/s) or stagnant conditions.

Hydrogen sulphide corrosion was not considered a viable corrosion mechanism for this pipeline. H_2S is more often associated with cracking than metal loss corrosion and at a partial pressure of 2.8×10^{-5} MPa, H_2S cannot generate metal loss corrosion rates of circa 1 mm/year[1].

The most likely failure mechanism was therefore considered to be CO_2 corrosion. Whilst it was not possible to verify this after-the-fact, comparison of the failure rate with established CO_2 corrosion rate prediction models supported the hypothesis. BP uses a modified de Waard & Milliams methodology[1,2,3,4] to predict CO_2 corrosion rates and for the Wytch Farm conditions, the predicted rate is 1 mm/year, agreeing well with the failure rate (7.8 mm wall thickness, failed after 7 years service).

The Wytch Farm produced water is unusual for oilfield brines in containing only 40 ppm of bicarbonate (HCO_3^-), rather than the more typical range of 500 - 2500 ppm. This, together with a high concentration of acetate ($CH_3CO_2^-$) at 100 ppm resulted in a relatively low pH of 4.5, thereby increasing the CO_2 corrosion rate[5].

Finally, support for the CO_2 hypothesis came from laboratory corrosion tests on separated produced water samples. Simple bubble tests[6] were performed under CO_2-saturated conditions and the corrosion rate observed agreed well with that predicted from the failure rate and BP corrosion rate prediction model[1].

ANALYSES RELATING TO METALLURGY

Linepipe Corrosion

The intelligent pig inspection report for the 10" pipeline reported a total of 281 metal loss defects. The majority of these were internal metal loss, generally located around the 6 o'clock position on the pipe. There were a small number of internal and external manufacturing defects reported, and a small number of external corrosion defects. In total, 246 linepipe features were considered as internal corrosion for the purposes of the work. The maximum reported feature depth was 79% of wall thickness (confirmed by excavation and UT measurement), although typical pit depths ranged between 10% and 70% of wall thickness. The majority of pits were less than 30 mm in length (measured along the axis of the pipeline).

The distribution of corrosion features with respect to the distance along the pipeline, circumferential position and linepipe steel grade is shown in Figure 4.

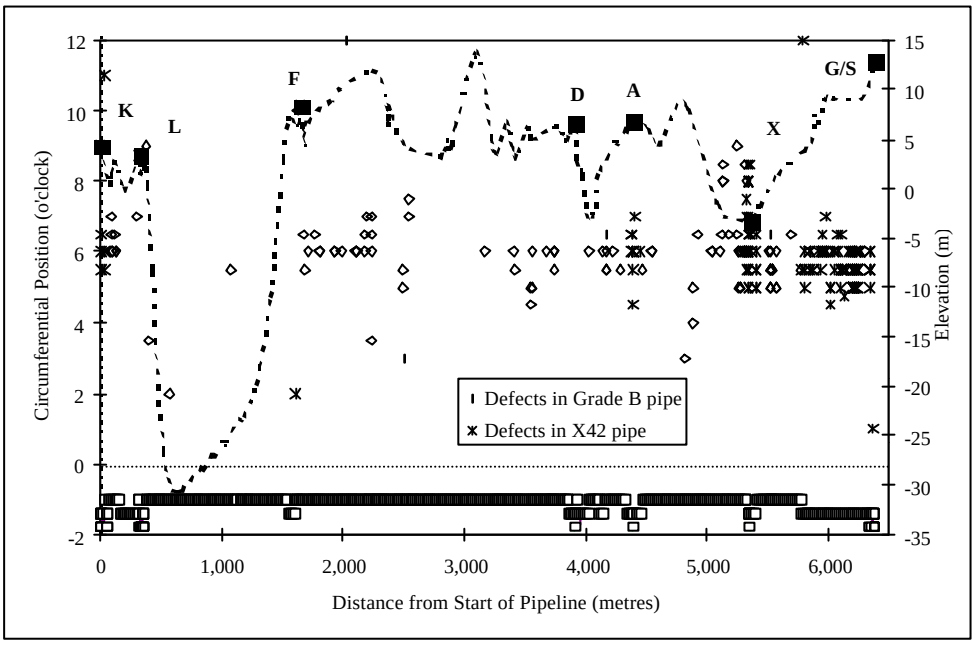

Figure 4: Distribution of pipebody corrosion features and corresponding linepipe steel grade

The distribution of linepipe steel grades (from the as-built records) is shown along the bottom of the chart (with a nominal negative y value), plotted in the order Grade B, X42 unknown from top to bottom. (There were a small number of pipes/welds for which no records could be found). X52 bends, and pipe of unknown grade/origin are few in number and do not feature any linepipe defects, and so were not considered in the analyses.

As shown in Figures 2 , the corrosion pit frequency increases downstream of Wellsite X. This is an area with a high proportion of X42 pipe, but it is also an area known to have a harsher flow regime than the rest of the pipeline. The effects of flow regime are discussed later in this paper.

Analysing the linepipe corrosion trends quantitatively and with respect to steel grade and location in the pipeline (either upstream [K-X] or downstream [X-GS] of Wellsite X), the results are quite clear: X42 linepipe is more susceptible to corrosion than Grade B linepipe (over both regions); and, corrosion is significantly increased downstream of Wellsite X (for both steel grades). There is also a relationship between the defect profile and the steel grade. The results of the analyses are presented in Table 4 and Table 5.

TABLE 4
LINEPIPE DEFECT DATA

Steel Grade/ Location	Frequency of Defects (per 100 m)	Mean Defect Depth (mm)	Mean Defect Length (mm)	Mean Defect Aspect Ratio	Mean Defect Area (mm^2)*
Gr B (K-X)	1.9	1.56	19.7	0.129	29.0
X42 (K-X)	8.1	1.84	15.1	0.191	24.5
Gr B (X-GS)	4.8	1.47	15.6	0.136	22.2
X42 (X-GS)	14.7	2.26	15.6	0.246	28.4

* Defect Area refers to the cross sectional area of the feature, i.e. the product of the depth and length.

Table 4 shows that the corrosion defects in the upstream and downstream locations (low fluid velocity and high fluid velocity respectively) are similar when considering the same grade of linepipe, i.e. the mean defect depths, lengths, aspect ratios and areas are essentially constant for a given grade of steel. It is the frequency of defects that increases significantly in highly turbulent flow.

TABLE 5
RATIOS OF DEFECT FEATURES BETWEEN STEEL GRADES AND PIPELINE LOCATIONS

Ratio	Frequency of Defects	Mean Defect Depth	Mean Defect Length	Mean Defect Aspect Ratio	Mean Defect Area*
X42 : Gr B (K-X)	4.25	1.18	0.76	1.49	0.84
X42 : Gr B (X-GS)	3.07	1.54	1.01	1.80	1.28
X-GS : K-X (Gr B)	2.53	0.94	0.79	1.06	0.76
X-GS : K-X (X42)	1.83	1.23	1.04	1.28	1.16

* Defect Area refers to the cross sectional area of the feature, i.e. the product of the depth and length.

Table 5 shows similar data to Table 4, expressed as ratios of the performance of X42 and Grade B and the ratios for upstream and downstream of wellsite X. It shows that X42 linepipe has 3 to 4 times the corrosion frequency of the Grade B pipe, upstream and downstream of Wellsite X. Both steel grades see approximately twice the frequency of corrosion downstream of Wellsite X (2.53 for Grade B and 1.83 for X42). Defect depths are greater in the X42 linepipe than Grade B at both locations, although there is less variation in defect length with respect to either steel grade or pipeline location.

It should be noted that these results do not include an allowance for the measurement tolerance of the intelligent pig. These are assumed to be negated by the number of features under consideration, and since the analysis is considering comparatives, the effects of tolerance are further reduced. Also, a limited number of UT measurements on linepipe defects confirmed the pig results to be accurate.

Aspect ratio is the ratio of defect depth to length and thus gives an indication of the profile of the defect: larger numbers indicate shorter, deeper pits; smaller numbers indicate longer shallower defects. X42 linepipe clearly shows larger aspect ratios (deeper pits) than the Grade B pipe in both sections of the pipeline, although it is interesting to note that the overall area of metal lost to corrosion varies only slightly with steel grade and location.

The increased frequency of defects in X42 and Grade B line pipe downstream of Wellsite X, in itself does not necessarily lead to pipeline failure (through leakage). However, given a particular distribution curve 'shape' (in this case for defect depths), an increased number of defects will give rise to an increased probability that one (or more) of the critical defects will be present.

The distributions of linepipe defect depths are shown in Figure 5. It can be seen that as the total number of defects increases, so too does the horizontal extent of the distribution increases (i.e. the standard deviation increases). Thus, because there are more defects in one type of pipe in one location, there is a higher probability that one or more of these defects will exceed some critical value.

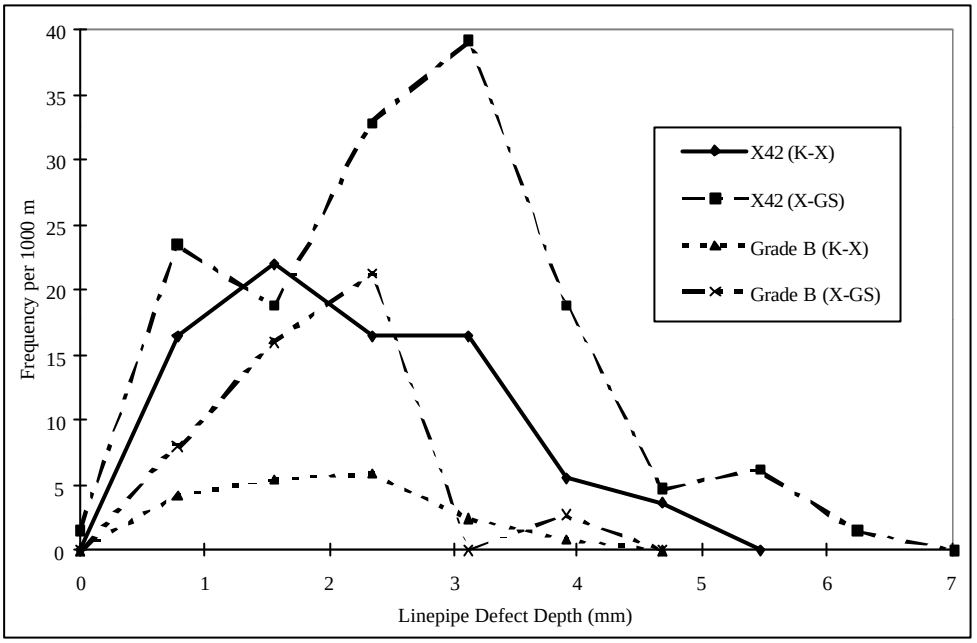

Figure 5: Linepipe defects depths for different linepipe steel grades and pipeline locations

It should be noted that the frequency of defect depth occurrences has been 'normalised' with respect to linepipe length to account for the differing quantities of the two linepipe steel grades situated in the two sections of the pipeline.

Weld Corrosion

As with the linepipe corrosion, the frequency and severity of corrosion damage was seen to increase towards the Gathering Station. Analyses similar to those conducted for the linepipe features were conducted for the weld defects (using the data acquired from the NDT programme and the pigging vendor analyses) with respect to the installation contractor responsible for completing the welds (and hence the weld procedure/material) and the grade of parent plate.

Note: the original site of pipeline failure was at a girth weld between a linepipe spool and a cast steel valve body. As this was not representative of the metallurgy or flow regime of the remaining girth welds, this weld was not considered in any of the analyses.

As the excavations and NDT examinations only covered about 30% of the welds on the pipeline (193 welds were subject to NDT out of 637 welds reported by the pig inspection), it was necessary to use the pigging vendor weld corrosion categories to supplement the NDT results. The semi-quantitative defect categories makes detailed analysis extremely difficult. To overcome this problem, the categories were simplified to a single depth value: where a range of depths were reported, the mean value was taken; and where the depth was noted as "greater than" a certain value, this value itself was taken as the depth. Although this last assumption may appear non-conservative, study of those estimates which have been subject to NDT shows that, where "greater than" statements are made, the measured depths have been both greater than, equal to, and less than, the estimated values. It should also be noted that all of the weld defects estimated by the pigging vendor to be deeper than 25% wall loss were excavated for NDT.

The pigging vendor was unable to comment on some of the welds reported by the intelligent pig inspection - these are primarily welds associated with Tee pieces and at anchor flanges, which are reported as welds by the pig, but cannot readily be described or analysed as "linepipe girth welds". There are also a number of areas on the pipeline where the installation contractor is unknown. All of these areas are small and are located at wellsites. Welds which did not have a quantified defect

depth (either estimated by the pigging vendor or measured by NDT), or which could not be attributed to an installation contractor were removed from the analysis process. Therefore the number of welds analysed was 585.

Weld Performance with Respect to Installation Contractor Only When weld performance was measured with respect to each of the three installation contractors, information was gained on:

- The total number of welds performed by each contractor.
- The number of 'defective welds' attributed to each contractor (and thus the percentage of welds completed by each contractor which are defective).
- The mean depth of weld defects attributed to each contractor.

This information is presented in Table 6.

TABLE 6
WELD CORROSION PERFORMANCE BY INSTALLATION CONTRACTOR

Installation Contractor	Total Number of Welds	Number of 'Defective' Welds	Percentage of Welds 'Defective'	Mean Corrosion Defect Depth (% Wall Thickness)
Contractor A	288	123	42.7	37.6
Contractor B	100	2	2.0	25.0
Contractor C	197	3	1.5	15.0

As can be seen, welds by Contractor A suffer significantly more corrosion (both in terms of depth, and the percentage of 'defective' welds), than welds by either of the other two installation contractors. Although this might suggest that welds by Contractor A may be more susceptible to corrosion because of some factor peculiar to their welding process (such as the weld procedure or consumables), there are other, more probable explanations for the different performances. These are discussed in detail below.

Additionally, the weld consumable used by Contractor A was the same type (C-Mn) as that used by Contractor C, whose welds feature substantially lower corrosion susceptibility. This further tends to rule out the installation contractor as a variable in weld corrosion performance. Contractor B used a weld consumable containing 1% Ni but there is insufficient data to determine if this had a significant influence on the good corrosion resistance of the welds completed by Contractor B.

Weld Performance with Respect to Pipeline Location Flow regime, as discussed later in this paper, is shown to affect linepipe corrosion pit frequency and it is reasonable to assume that the flow regime influence on corrosion rates applies to weld corrosion as well. In fact, it is possible that the effect is even compounded at welds because of increased, highly localised turbulence caused by the uneven weld surface. This effect is discussed later.

The weld defect depths are plotted against distance along the pipeline in Figure 6. This Figure shows essentially the same information as Figure 3 but with the weld defects sub-divided to show the associated linepipe steel grade and installation contractor responsible for completing that particular section of the line.

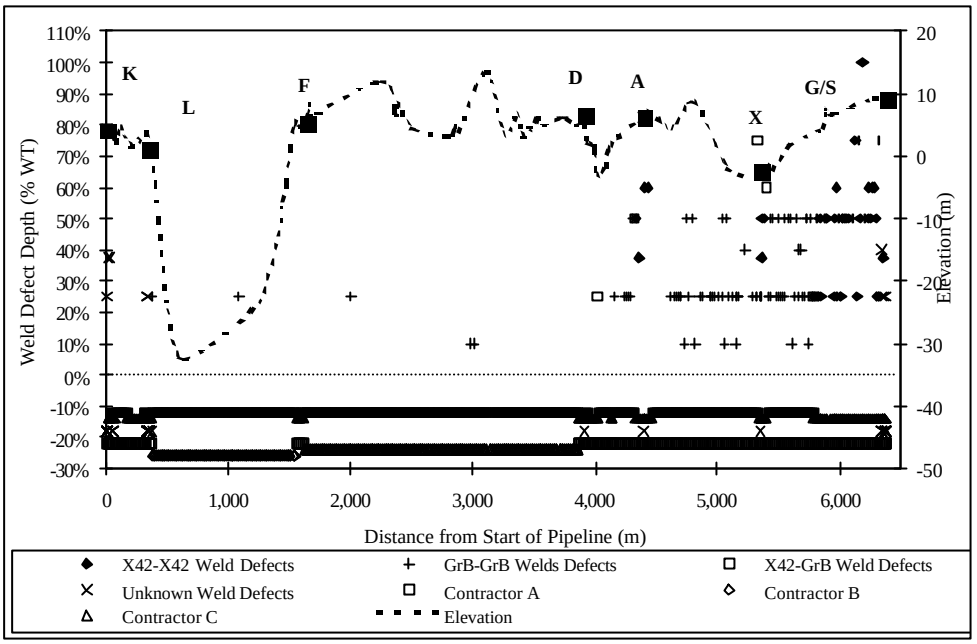

Figure 6: Details of defective welds by material type and contractor

Note 1: The data plotted between the lines y = minus 10% and y = minus 20% shows the linepipe steel grade. The upper of the two lines indicates GrB:GrB welds and the lower, X42:X42 welds.

Note 2: The data plotted below the line y = minus 20% shows the installation contractor, plotted in the order Contractor A, C, B from upper to lower. Also plotted on the Figure are the pipeline elevation and the locations of the various wellsites.

It can be seen that the density of defective welds increases dramatically downstream of KP 4 - approximately the location of Wellsite D (for clarity, this section of the line is re-plotted in Figure 7, showing the same data as is shown in Figure 6, except the installation contractor information is omitted). For this reason, similar analyses to those conducted over the whole pipeline showing the performance of welds by different installation contractors were conducted for the sections of pipeline upstream and downstream of Wellsite D. The results are presented in Table 7 and Table 8 below.

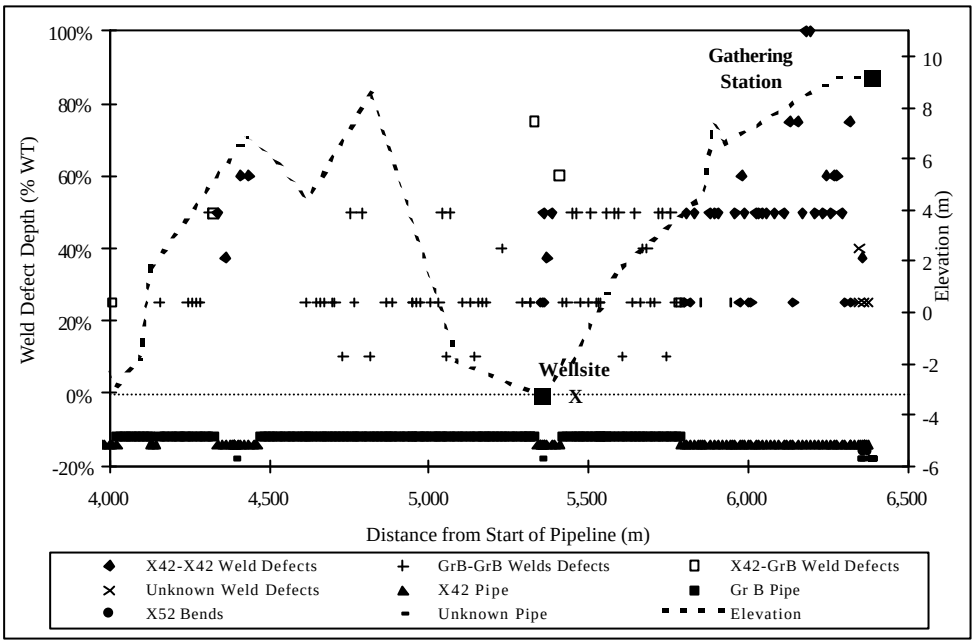

Figure 7: Details of defective welds by material type from KP 4 to the Gathering Station

TABLE 7
WELD PERFORMANCE BY INSTALLATION CONTRACTOR, UPSTREAM OF WELLSITE D

Installation Contractor	Total Number of Welds	Number of 'Defective' Welds	'Defective' Welds Percentage	Mean Corrosion Defect Depth (% Wall Thickness)
Contractor A	60	2	3.33	37.50
Contractor B	100	2	2.00	25.00
Contractor C	197	3	1.52	15.00

TABLE 8
WELD PERFORMANCE BY INSTALLATION CONTRACTOR, DOWNSTREAM OF WELLSITE D

Installation Contractor	Total Number of Welds	Number of 'Defective' Welds	'Defective' Welds Percentage	Mean Corrosion Defect Depth (% Wall Thickness)
Contractor A	228	121	53.07	37.62
Contractor B	0	0	N/A	N/A
Contractor C	0	0	N/A	N/A

It can be seen that the majority of 'defective' welds are downstream of Wellsite D, and that all of the welds in this section of pipeline were completed by Contractor A. Thus any flow regime effects which may exist towards the downstream end of the pipeline will act to adversely affect the perceived corrosion performance of welds by Contractor A.

It should be noted that any effects of parent pipe steel grade on corrosion susceptibility are also likely to influence the corrosion performance of the installation contractors. Since only Contractor A completed welds in X42 linepipe, the small number of defective welds completed by the other installation contractors makes any comparison of defect depths invalid.

Weld Performance with Respect to Parent Plate Steel Grade Consideration was given to the theory that the corrosion could be driven by galvanic interaction between linepipe of different steel grades. Analyses were subsequently performed to investigate this effect, the results of which are presented in Table 9 below.

TABLE 9
WELD CORROSION PERFORMANCE BY PARENT PIPE STEEL GRADE

Parent Plate Steel Grade	Total Number of Welds	Number of 'Defective' Welds	'Defective' Welds Percentage	Mean Corrosion Defect Depth (% Wall Thickness)
X42-X42	104	49	47.12	46.89
GrB-GrB	133	64	48.12	30.16
X42-GrB	22	5	22.73	47.00
Unknown/Other	29	5	17.24	33.00

These data are for welds completed by Contractor A only (which account for the vast majority of 'defective welds') both upstream and downstream of Wellsite D.

The table shows that there appears to be little difference between the corrosion susceptibility of welds when the parent pipe either side of the weld is of the same steel grade. Where the parent pipe is of different steel grade (or where one or both of the parent pipes are of unknown or other steel grades such as API 5L X52), the susceptibility appears to be much lower: however this may just be an effect of the lower quantity of data.

There would also appear to be an increase in the mean corrosion defect depth in X42-X42 welds over GrB-GrB welds. Where one of the parent pipes is X42, the defect depth is also seen to be greater than those in GrB-GrB welds, although as noted above this may be an effect of the lower quantity of data. Flow regime was noted not to have a significant effect on the depth of linepipe body corrosion features although a difference was noted in the mean depth of metal loss features between different linepipe grades.

There appears to be a correlation between the mean depth of the weld defects and the mean depth of features noted in the linepipe body. The results of the linepipe data analyses in Table 5 showed that at the downstream end of the pipeline, metal loss features in X42 linepipe were 1.54 times deeper than those in Grade B linepipe. The ratio of X42-X42 to GrB-GrB weld defect depths is calculated to be 1.55 from the data in Table 9. These ratios are almost identical, which further suggests a link between the steel grade and the corrosion rate.

The variation in corrosion depths between different linepipe grades may still be partially affected by the flow regime, since the majority of the X42 linepipe is in an area of more turbulent flow. However there is no way of confirming this affect without a more detailed model of the variation in flow regime along the length of the pipeline - see later.

The distribution of weld defect depths with respect to parent pipe steel grade is shown in Figure 8 for welds completed by Contractor A. In order to show the overall susceptibility to corrosion of welds between each parent pipe combination, the distribution shows the number of weld defects falling into each depth 'band' per 100 welds.

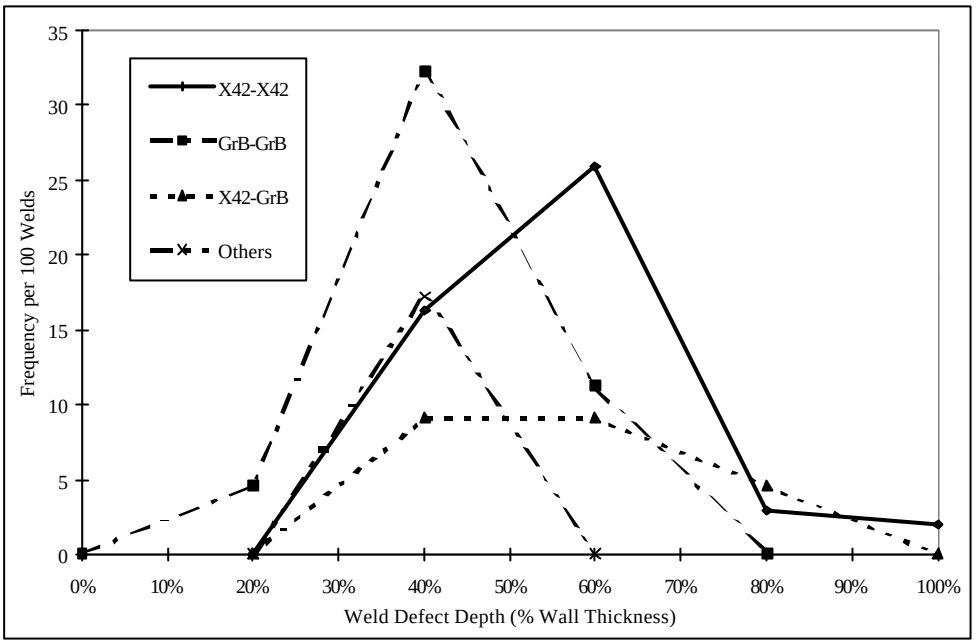

Figure 8: The Distribution of Weld Defects Depths for Different Parent Pipe Steel Grades

Clearly the X42-X42 welds show a trend towards deeper corrosion defects, which is in agreement with the greater mean defect depth which these welds are seen to exhibit.

The two welds which show 100% wall thickness defects comprise the second 'in-service' failure, and one weld which failed during shot blasting to remove the coating prior to NDT. The first 'in-service' failure is not presented in these results for the reasons mentioned earlier.

It should be noted that, aside from corrosion susceptibility, only the weld defect depths have been evaluated. There were insufficient data available, either from the pigging vendor estimates or from the NDT, to enable information on the area, volume or aspect ratios of metal loss at welds to be processed.

ANALYSES RELATING TO FLOW REGIME

Influence of Flow on Corrosion

It has long been established that flowrate has an effect on corrosion rate, both in single phase and multiphase flows, but only in recent years has dedicated research been performed in this field[7, 8]. This is particularly true in the area of multiphase flow, which is generally the area of most interest to producing oil fields, where infield pipelines carry untreated multiphase mixtures of oil, water and gas.

Recent work by Ohio University and the Institute for Energy in Norway has indicated strong correlations between corrosion rates measured on a test rig and the type of flow regime observed[7, 8]. In the Ohio work, a modified Froude number is related to corrosion rates and this approach is adopted here. A definition of the Froude numb er is given by equation 1.

Nature of Froude Number The Froude number is a measure of the turbulence induced into the film in front of a slug as it moves over the liquid film. Corrosion is enhanced as the boundary layer is thinned and is eventually destroyed by increasing slug velocity and the decreasing of liquid film thickness. It follows that the Froude number is higher going up hill than it is downhill for similar flow rates of oil, water and gas as the film is thinner uphill (liquid hold-up is reduced due to the affects of gravity).

The Froude number form of analysis is based on idealised pipelines, i.e. smooth, constant diameter pipes with no intruding fittings or junctions. The affects of disruptions to flow path on the turbulence at the front of a slug, are therefore not well understood. Current understanding recognises that these effects give rise to localised turbulence which increases significantly around small intrusions, such as welds. Unpublished work based on mass transport experiments and computational fluid dynamics modelling has shown local shearing effects to be double or greater the shear seen in normal flow.

Figure 9. shows a possible affect of an intrusion (such as a weld root) on the corrosion rate and its possible relationship to the Froude number. It should be noted that the shapes of the curves are only approximate and not based on highly detailed analysis. The rate of corrosion is shown on the Y-axis of the trend chart and demonstrates the two extremes of corrosion.

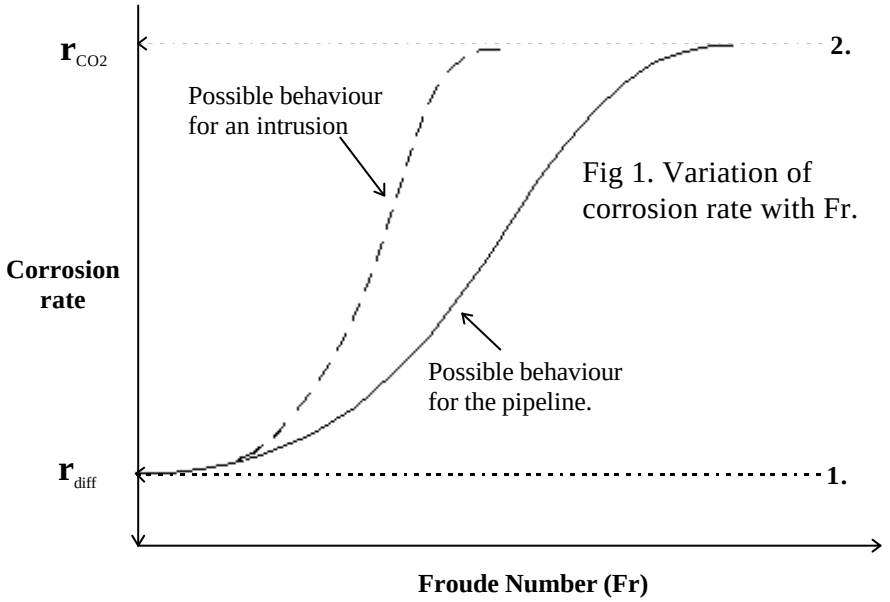

Figure 9: Possible relationship between Froude Number and corrosion rate

Diffusion rate controlled Corrosion Line 1 in Figure 9: the rate of diffusion is controlling the corrosion rate. Rate of reaction is r_{diff} The reaction is limited by the mass transfer to or from the surface. i.e. the rate of diffusion through the lamina sub-layer and buffer zone is slow in comparison to the reaction rate at the surface.

Reaction rate controlled Corrosion Line 2 in Figure 9: The rate of reaction is controlling the corrosion rate. Rate of reaction is r_{CO2}. i.e. the turbulence generated by the flow completely removes the diffusion effect which would otherwise limit the reaction rate.

Most field conditions will be between the two extremes, where the boundary layer plays a role in determining the corrosion rate. This is the approach taken in a recent corrosion rate prediction model[4]. Recent work has attempted to define the level of turbulence required under multiphase flow to cause a significant shift in the corrosion rate, from that being dominated by diffusion control to a much higher rate, dominated by reaction kinetics[7]. For CO_2 corrosion under multiphase slug flow, the Froude number range of 5 to 8 was defined[7] as the critical range over which this transition takes place.

This assumes that there will be free water available to wet the pipewall and cause corrosion. The approach used, following the procedure of Karabelas[9], was to establish if water is in a free state, using a critical close packing criteria where, once the water concentration exceeds a critical value, it is assumed to coalesce and form a continuous phase.

General Modified Froude Number Calculation

This calculation is based on numerous pieces of work in multiphase flow and ultimately yields a modified Froude number, first proposed by Jepson[5]. This modified Froude number (Fr) is of the form:

$$Fr = \frac{V_S - V_F}{\sqrt{gD_e}} \tag{1}$$

Where V_S is the slug translational velocity, typically of the form

$$V_S = kV_M + C \tag{2}$$

and where V_F is the film velocity, V_M is the mixture velocity, g is gravity, D_e is the effective height of the film and C is a constant. The key to the calculation is to obtain the variable D_e which is dependant on the film hold up amongst other things.

$$D_e = \frac{A_L}{2\sqrt{D_i^2 H_F - H_F^2 D_i^4}} \tag{3}$$

From Geometry:

$$A_L = \frac{D_i^2}{4}\cos^{-1}\left(\frac{D_i^2 - 2H_F}{D_i}\right) \tag{4}$$

Here A_L is the area the liquid occupies and D_i is the internal diameter of the pipeline, the variable H_F is the hold up in the film. H_F features in both equations 3 & 4, but is also a key factor in finding V_F. To find V_F a simple mass balance over a slug bubble unit yields the following relationship.

$$V_F = \frac{V_{SL} H_L (L_S + L_B) - H_{LS} V_M L_S}{L_B H_F} \tag{5}$$

H_L is the hold up on average in a section of pipe and can be obtained from Taitel Dukler's[10] method of interfacial friction balancing, where:

H_{LS} is the hold up in a slug (obtained from a suitable correlation)
V_M is the mixture velocity
V_{SL} is the superficial gas velocity.

The slug and bubble lengths, L_S and L_B can be found from a mass balance, once the slug frequency has been calculated using an appropriate correlation. These methods are widely available.

Finally a closure relationship is required to link H_F and V_F (notice that any pair of these numbers can satisfy equation 5). There are several methods available to provide this relationship, some of which are highly iterative. It is recommended to use the Crowley[11] method to calculate the hold up in the film.

Application to this Case Study

In order to quantify the influence of flow on the observed distribution and severity of corrosion in the Wytch Farm pipeline, production data for the previous 2.5 years was taken, (averaged on a monthly basis) and predictions of nodal pressures were

calculated using a matched multiphase flow spreadsheet which provided physical properties at each point. Each node is one of the topographical points shown in Figure 1, where a change in inclination takes place.

The presence of free water in large parts of the pipeline is known from the observed corrosion damage, but checks were performed, using the method of Karabelyas, to establish if there were limits to where a free water layer will exist. The outcome was that a free layer of water is found along the length of the pipeline, confirming the widespread corrosion damage found by the intelligent pig. The Froude number was calculated for the pipeline to determine if it could explain the pattern of corrosion damage observed.

The general approach described above was applied with the following simplifications and closure relationships:

- A slug shedding factor of 1.25 was used, i.e. k=1.25 with C=0
- H_{LS} was calculated using Gregory[12]
- Inclination was ignored because of the varied results obtained in Slug Frequency calculations. Hill et al[13] was used to describe horizontal slugs.
- The approach of Crowley was used to calculate H_F and Tiatel Dukler to obtain the equivalent stratified layer hold up.

Figure 10 shows the variation of Froude number with distance along the pipeline for a sample month, in this case January '97.

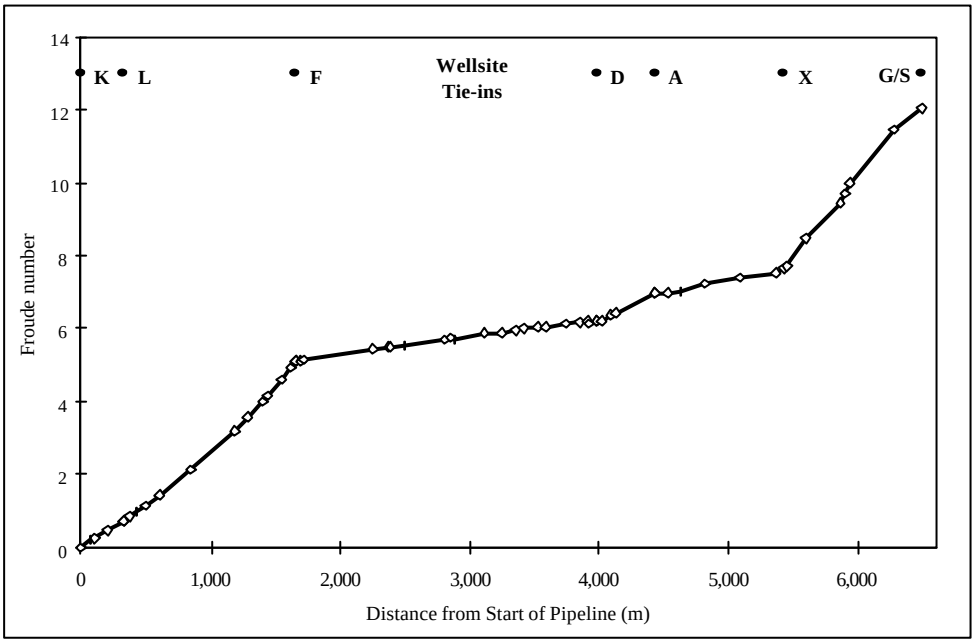

Figure 10: Variation of Froude number along the length of the pipeline.

As Figure 10 shows, there is a sudden increase in Froude number beyond the last tie in point, Wellsite X. This is mainly due to the rapidly increasing pressure drop due to the incline up to the Gathering Station, rather than large volumes of fluid entering at this point. As the velocity increases (driven by the gas expansion), the slugs accelerate, which in turn increases the overall pressure drop further as the localised pressure drop over a slug is higher than for other feasible flow regimes.

If all the historical data is put through the same process and the Froude number at each tie in point is considered then Figure 11 is obtained. This Figure shows that the flow regime at each tie-in point has been approximately constant, with only minor variations in Froude number over time.

From multiphase flow modelling, the predominant flow regime is slug flow in the horizontal and uphill sections. As the Froude number is a measure of turbulence at the front of a slug, Froude number can be used as a measure of the turbulence in these sections.

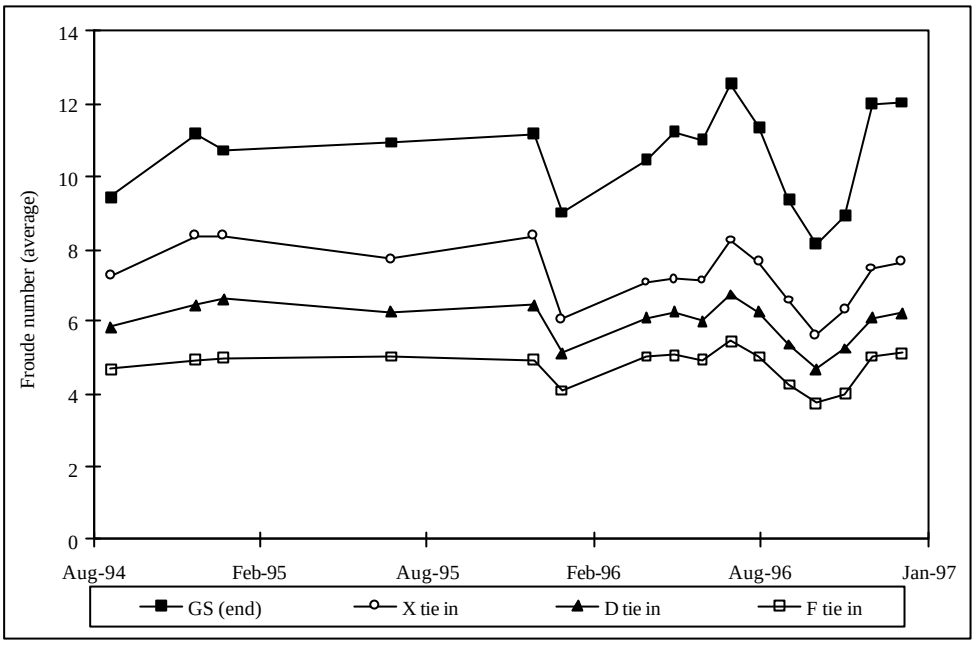

Figure 11: Variation of Froude Number over time at tie in points.

From this work, it can be seen that the majority of the pipeline (from KP 1.8 to the end) is operating at Froude numbers greater than 5 but only the final section (corresponding approximately to the X-site tie-in or KP 5.3) is operating at a Froude number greater than 8. From the observations made regarding the frequency of corrosion defects in the linepipe, it appears that Froude numbers greater than 8 are required to significantly increase the frequency of corrosion defects on a smooth pipe.

The observations made regarding girth welds showed that the frequency and rate of corrosion at welds increased further upstream than did the linepipe corrosion frequency (corresponding to wellsite D, or KP 4.0). From this, it can be postulated that the localised turbulence at a weld root is equivalent to an overall increase in Froude numbers of 2 or 3 above that predicted for smooth pipe. Localised mass transfer coefficients in single phase flow downstream of a 2mm weld bead are approximately twice that in the equivalent smooth pipe at 2 m/s full pipe flow velocity[14].

SUMMARY & CONCLUSIONS

The frequency of corrosion in linepipe is seen to increase at the downstream end of the pipeline regardless of the linepipe steel grade. This area corresponds with more aggressive flow regimes, which have been shown experimentally to induce higher corrosion rates. Although the individual pit corrosion rates seen in linepipe at the downstream end of the pipeline are no greater than at the upstream end, the increased frequency of similarly dimensioned corrosion pits is evidence of an increase in the overall rate of metal loss. This implies that the corrosion process is determined by a cathodic reaction i.e. under highly turbulent flow, more anodic sites (pits) can be supported per unit area while the rate remains constant. The greater frequency of pits in linepipe in the downstream section results in an increased probability that a defect of critical depth will be present.

The situation is similar for welds, but in this case there is an increase in both frequency and depth of corrosion in the downstream section of the pipeline. The almost total absence of corroded welds in upstream sections indicates that they may be protected, possibly by surface films or a galvanic affect. However, once the flow regime is turbulent enough to initiate corrosion in the welds, the rate of pit growth and frequency of attack increase markedly.

Corrosion rates are seen to be increased in X42 linepipe and in X42-X42 welds when compared with Grade B linepipe and Grade B - Grade B welds, both in areas of harsh flow regime and areas of relatively non-aggressive flow. Metallurgy is thus shown to have an influence on the corrosion behaviour of the pipeline, even for steels with similar chemical compositions, mechanical properties and manufacturing routes.

Corrosion rate prediction models and simple laboratory simulations of field conditions have been shown to give an accurate estimate of in-situ corrosion rates for this case study. Care needs to be taken when carrying out such work to ensure that all the important fluid properties are considered as apparently minor changes in fluid composition, namely bicarbonate and acetate concentrations can have a marked affect on the outcome. However, a word of caution is necessary when using laboratory generated corrosion rates. They tend to be generated using electrical resistance (ER) or linear polarisation resistance (LPR) probes (LPR in this case) and therefore assume uniform corrosion. As this paper shows, high flow rates may increase the number of corrosion pits but not necessarily the corrosion rate. ER and LPR probes (when used in the normal manner) would show this as an increase in corrosion rate. It is therefore important to use a suitable flow rate and flow regime when generating quantifiable corrosion rates in the laboratory. When the data are used qualitatively, for ranking purposes such as in corrosion inhibitor selection studies, this is not a major concern.

Simple corrosion rate prediction models are often used as the basis for calculating critical variables such as mean time to failure, or probability of failure in a risk-based approach. This work shows that corrosion rate and corrosion pit frequency are controlled by a combination of fluid properties, metallurgy and flow regime and simple corrosion rate prediction models are incapable of satisfactorily dealing with these factors.

REFERENCES

1. A. J. McMahon and D. M. E. Paisley, "Corrosion Prediction Modelling", BP Guidelines, Report number ESR.96.ER.066, November 1996.
2. C. de Waard, U. Lotz, and D. E. Milliams, "Predictive model for CO_2 corrosion engineering in wet natural gas pipelines", Corrosion, 47 (1991) 976.
3. C. de Waard and U. Lotz, "Prediction of CO_2 corrosion of carbon steel", NACE Corrosion 93, New Orleans, Paper 69.
4. C. de Waard, U. Lotz and A. Dugstad, "Influence of liquid flow velocity on CO_2 corrosion: A semi-empirical model", NACE Corrosion 95, Orlando, Paper 128
5. B Hedges, L. McVeigh "The Catalytic Role of Acetates in CO_2 and the Acetate Double Whammy" NACE Corrosion 99
6. S. Webster, A.J. McMahon, D. M. E. Paisley and D. Harrop, "Corrosion inhibitor test methods", BP Guidelines, Report number ESR.95.ER.054, November 1996.
7. P Jepson et al. National Science Foundation Industry/University Co-operative Research Centre for Corrosion in Multiphase Systems, Ohio University
8. S Nesic, M Langsholt, K Lunde, M Nordsveen, D Thomassen "The Effect of Multiphase Flow on CO_2 Corrosion and its Inhibition: Phase I - Measurements of Wall Shear Stress and Mass Transfer in Two-Phase Gas/Liquid Flow" IFE/KR/F-95/205. Unpublished work by IFE for BP, and Statiol
9. Karabelas, A.J. Vertical Distribution of Dilute Suspensions in Turbulent Pipe Flow AIChemE Journal (Vol23, No. 4) July 1977.
10. Taitel, Y. & Dukler, A.E. 1976, A Model for Predicting Flow Regime Transitions in Horizontal and Near Horizontal Gas-Liquid Flow AIChE Journal, Vol 22, 47-55.
11. Crowley, C.J. & Rothe, P.H. 1986 State of the Art Report on Multiphase Methods for Gas and Oil Pipelines volume 2 Guide to Computerised Calculations Creare Inc. report TN-409 vol. 2 (prepared for Project PR-172-609, American Gas Association, Catalog No. L51527).
12. Gregory, G.A., Nicholson, M.K. & Aziz, K. (1978) Correlation of Liquid Volume Fraction in the Slug for Horizontal Gas - Liquid Slug Flow Int J Multiphase Flow, 4, 33-39
13. Hill, T.J. and Wood, D.G Slug Flow: Occurrence, Consequences and Prediction paper SPE 27960 presented at the University of Tulsa Centennial Petroleum Engineering Symposium, 29-31 August 1994.
14. Lei Jang Advisory Group Meeting Report, October 1997 National Science Foundation Industry/University Co-operative Research Centre for Corrosion in Multiphase Systems, Ohio University